



## Mechanical aspects of nitrile hydratase enzymatic activity. Steered molecular dynamics simulations of *Pseudonocardia thermophila* JCM 3095

L. Peplowski, K. Kubiak, W. Nowak\*

Theoretical Molecular Biophysics Group, Institute of Physics, N. Copernicus University, Grudziadzka 5, 87-100 Torun, Poland

### ARTICLE INFO

#### Article history:

Received 4 June 2008

In final form 27 October 2008

Available online 5 November 2008

### ABSTRACT

Nitrile hydratase (NHase), an important biotechnological enzyme, has been investigated using a steered molecular dynamics computer modelling for the first time. An external force applied to the docked ligands was used to determine transport paths for acrylonitrile (substrate) and acrylamide (product). The average drag force of 120 pN within the enzyme channel is 50% higher than that in model water. The major hindrance of 500 pN is generated by  $\beta$ Phe37 residue. This region may be responsible for the stereoselectivity of NHases.

© 2008 Elsevier B.V. All rights reserved.

### 1. Introduction

Mechanical properties of biomolecules are of great interest because they govern the shape of living organisms and provide boundary conditions for all biochemistry [1]. The response of representative proteins to external mechanical stress has been studied using simple physical models [2,3]. Mechanically stretched single structural proteins, such as titin or ankyrin, have been investigated on a single molecule level using experimental techniques, as well i.e. atomic force microscope (AFM) [4,5]. The recently developed computational technique of steered molecular dynamics (SMD) is a useful tool in biophysics, complementary to single molecule level manipulation methods [6,7] such as AFM or optical tweezers. In the SMD method [8] effects of an external force applied to a critical part of a biopolymer are traced using numerical solutions of Newton's equation of motions. The biomolecule is modelled by a set of point masses coupled by appropriate interaction potentials. The formalism and recent progress of the single molecule SMD method have been recently reviewed [7,9,10]. Its advantages have been shown in studies of mechanical properties of oligosaccharides [9–12] and sugar transport through protein pores [13], titin [14–16] or mechanoselective channels [7]. However, in contrast to relatively well studied structural proteins, enzymes were rarely probed using AFM or SMD methods.

The first ligand–protein binding SMD-type study was published by Grubmuller et al. already in 1996 [17]. In 1999, Kosztin et al. used SMD to probe retinoic acid hormone release from a model of nuclear receptor [18]. Gerini et al. investigated forced unbinding of veratryl alcohol from lignin peroxidase [19]. Shen et al. used

the SMD method to compare binding properties of prospective drugs towards HIV-1 reverse transcriptase [20]. Wade proposed a very interesting method of random expulsion molecular dynamics (REMD) to identify potential substrate and product egress pathways in cytochrome P450 [21]. Very recently Liu et al. used genetic algorithms to search optimal pulling directions in SMD substrate unbinding in cytochrome P450 complex [22], but the optimised maximal forces were only marginally lower than those obtained in a standard SMD simulations.

In principle, one can use an external force to probe ligands' paths inside a protein matrix. Such an approach helps to identify transport routes and molecular control points. In this paper, we investigate interactions of substrates and products of industrial enzyme nitrile hydratase [23] for the first time.

Nitrile hydratase is a metalloenzyme used for large scale industrial production of important commodities such as acrylamide and nicotinamide [23,24]. The mechanism of its activity is not yet known, despite many quantum mechanical studies of model active sites [25–29] and mimetic compound studies [30]. Selectivity of NHase towards substrates with varying size and space arrangements is the subject of both experimental [31–33] and theoretical studies [34,35]. In order to identify sources of molecular friction during the forced motion of a large ligand in a protein matrix, we used the SMD technique to study NHase from *Pseudonocardia Thermophila* JCM 3095 WT enzyme [33]. This is a system with high potential for bioindustrial applications. A series of 2 ns and 1 ns SMD simulations revealed the mechanical response of the enzyme to the enforced dissociation of two types of compounds. Important features of hypothetical classical reactions paths have thus been computationally determined for an enzyme used in biotechnology. Our approach opens the way to further nanomechanical studies of similar complexes as well as to the rational design of artificial enzymes.

\* Corresponding author. Fax: +48 56 6225397.

E-mail address: [wiesiek@fizyka.umk.pl](mailto:wiesiek@fizyka.umk.pl) (W. Nowak).

## 2. Materials and methods

Density Functional Theory with the B3LYP functional and the 6–311G\* basis set (DFT/B3LYP/6–311G\*) was used for the geometry optimization of the structures of acrylonitrile (ACN) and acrylamide (ACA). Dockings of the substrates and products to the crystal structure 1IRE of Co-NHase from *Pseudonocardia thermophila* JCM 3095 [33] were performed using AutoDock 3.0.5 [36] code as described in Ref. [37].

The SMD simulations were performed using NAMD 2.6 [38] with the Charmm27 [39] force field. Each protein–ligand complex was put into a water box  $73 \times 81 \times 74 \text{ \AA}^3$  with a layer of water of at least 7 Å in each dimension. A cutoff of 12 Å for non-bonded interactions was applied. We performed 100 ps of water equilibration, 1000 steps of minimization and 50 ps of heating from the 0 K up to 300 K before each main SMD simulation.

For every ligand three 2 ns and ten 1 ns long SMD simulations were carried out. The external force was attached to the center of mass of the ligand and the velocity of the SMD reference point was  $2 \times 10^{-5} \text{ \AA/timestep}$ . An external force constant of 4 kcal/mol/Å<sup>2</sup> was used. In order to obtain a better statistics, the direction of the external force, initially selected along the NHase channel, was slightly randomized in 1 ns SMD trajectories. The temperature was kept constant using the Langevin method. For each ligand the starting configuration in the main SMD simulation was the same. As a reference for the SMD analysis a set of 10 ns long 300 K (Langevin) classical MD trajectories of substrate (or product)–Co-NHase complexes were generated (results unpublished). In all simulations 1 fs integration timestep was used.

The Charmm27 compatible topology and parameters for a non-standard NHase center and ligands (ACN, ACA) were home-made using our DFT and/or HF calculated charges. Force constants were extrapolated from the standard Charmm27 parameters.

All graphical analysis was performed using the VMD code [40] and home-made tcl scripts.

## 3. Results and discussion

During an enzymatic catalytic cycle the molecules of the substrate must reach the NHase interior, then hydration reaction takes place in the deeply buried catalytic site. Eventually products leave the catalytic cleft. Experimental X-ray data [41] indicate that the transport of substrates/products takes place through the channel located at the interface of  $\alpha$  and  $\beta$  subunits, as postulated by Huang et al. [42]. The fold of NHase is shown in Fig. 1 and the green arrow

approximately shows the orientation of the channel. In Fig. 2 the main residues forming the channel are schematically presented. The distance from the NHase surface to the  $\text{Co}^{3+}$  center is about 15 Å. While the other possible ligand/product transfer routes can not definitively be ruled out [43], both X-ray analysis [33,44] and our recent Locally Enhanced Sampling MD simulations of the related Fe–NHase [29] indicate that this channel plays the major role in the NHase functioning.

It is worth to note that the details of the architecture of the channel interior may be responsible for the fine-tuning of certain NHases for stereospecific synthesis of pharmaceutical semi-products [45].

In order to determine which aminoacids hinder substrate/ligand transport in the NHase and which regions may discriminate NHase ligands with respect to their size and geometry, the external force was applied to ACN (or a product ACA). The ligands were docked first in the active site cavity using AutoDock software [37]. The direction of the applied force is shown in Fig. 1. This vector is oriented approximately along the channel axis, corresponding to channel entrance no. 3 as discussed in Ref. [43], this seems to be the most natural way for the transport of the ligands.

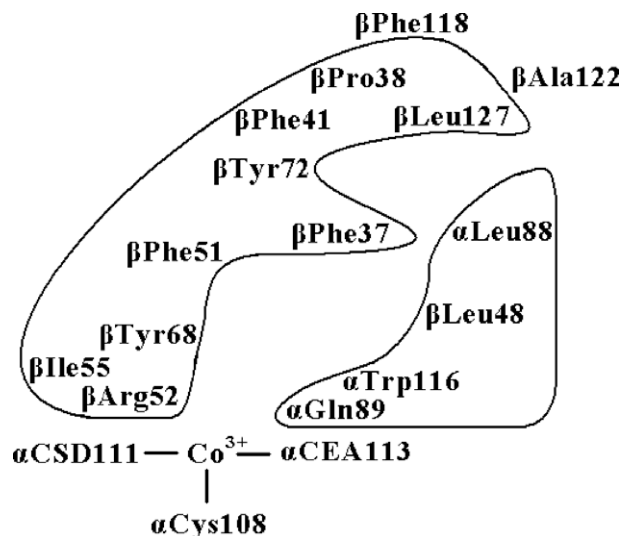


Fig. 2. A schematic view of the NHases channel. Only residues important for the ligand transport are shown. The exit is located near  $\beta\text{Ala122}$ .

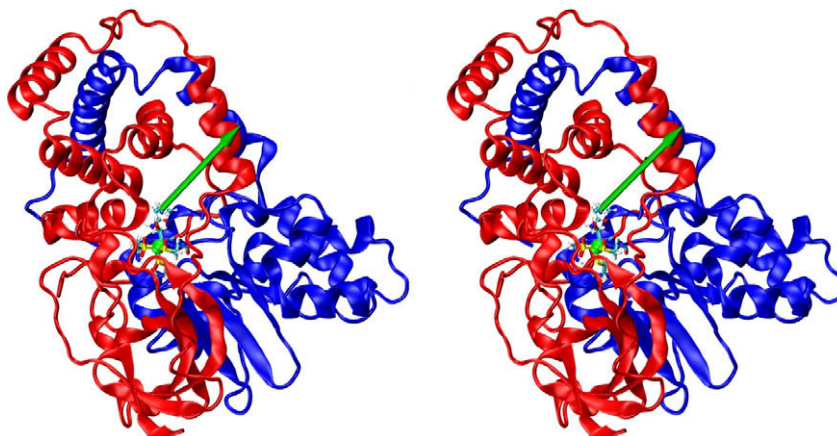
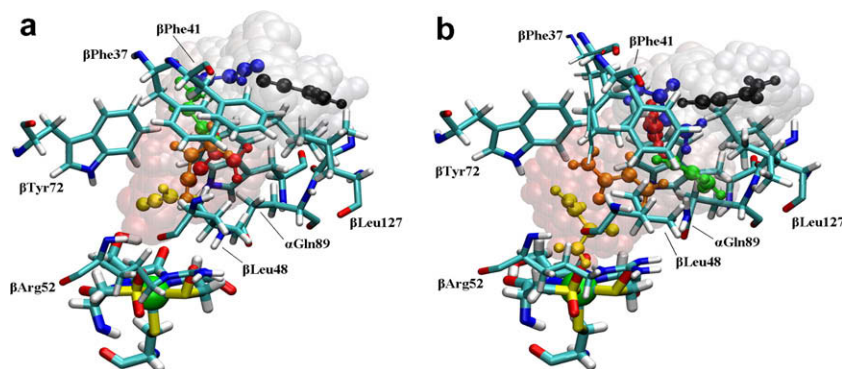


Fig. 1. A stereo view of NHase with the docked ligand and the main SMD pulling direction (green arrow). (For interpretation of the references to color in this figure legend, the reader is referred to the web version of this article.)



**Fig. 3.** Paths for **ACN** (a) and **ACA** (b) in SMD simulations. Note that in figure (b) two orientations of important  $\beta$ Phe37 side chain are shown.

Initially, three 2 ns trajectories have been obtained for each ligand, but closer analysis showed that after 1 ns of simulation the ligand had already reached the surface of the protein while during the last 0.8 ns the pulling took place in bulk water. Therefore the remaining simulations were restricted to 1 ns. One should note that the selected pulling direction, though in our opinion rational and justified by the structure of NHase, is an approximation of the real ligand diffusion process. One may expect that the direction of actual travel of substrates/products within the protein channel may vary from time to time during the catalytic cycle. In order to mimic this process we have randomized slightly the directions of the pulling force. The strict determination of the classical reaction coordinate for such a complex system as NHase is not possible. Alternative approximate methods, such as, random expulsion MD [21] or a very recently proposed the SMD with direction optimization [22] give only an estimate of upper limits for the possible steric hindrance present in a given enzyme.

All plots of force acting on the ligand with respect to a travelled distance (or simulation time) show similar qualitative character. Multiple minima (3–5) on all plots are observed. Representative data are shown in Fig. 3. The maximum force for each simulation of **ACN** pulling fluctuated between 223 and 457 pN. For the product (**ACA**) these values were in the range of 232–508 pN. The average force at the maximum was about 300–350 pN. The mean force during pulling the ligand in water was  $85 \pm 20$  pN. Rather low forces at maxima (140 pN above the drag force in water) indicate that steric hindrance from aminoacids forming the channel interior is not very severe. Our data show that the hindrance experienced by small nitrile substrates and amide products of NHase are quite similar.

Detailed paths from all simulations form a unified scheme. Typical paths are shown in Fig. 3.

Initially the ligand rests in the cavity above the enzymatic center (Fig. 3, yellow<sup>1</sup>). In some cases of **ACA** trajectories H-bonds with  $\alpha$ Gln89 are observed (Fig. 4b, maxima at 0.1 ns). A relatively low external force of 100–150 pN is tugging a ligand to  $\beta$ Phe37 and  $\beta$ Trp72 (Fig. 3, orange). The ligand stays there for about 200–400 ps. A strong interaction with  $\beta$ Phe37 manifests itself by a substantial growth of the force applied to the ligand up to 250–350 pN (see maxima at 0.3 ns in Fig. 4a and at 0.4 ns in Fig. 4b). Pulling the ligand causes a conformational change in CA-CB-CG-CD1 dihedral angle of  $\beta$ Phe37. This important conformational transition is shown in Fig. 2b, where two limiting conformations of  $\beta$ Phe37 side group are displayed. Plots of the relevant dihedral angle are pre-

sented in Fig. 4a and b. This enforced rotation requires the highest force observed in the whole SMD simulations of NHase. It is worth noting that in a classical MD simulation similar conformational changes of  $\beta$ Phe37 are also observed, but very rarely ( $1/6 \text{ ns}^{-1}$ ). We have noticed that the channel remains open for 30% of the MD simulation time.

After these steps the ligands stay between  $\beta$ Phe37 and  $\beta$ Phe41 for about 50–100 ps. From this ‘parking place’ ligands usually drift for a while into a pocket buried inside a protein matrix ( $\alpha$ Trp116,  $\alpha$ Val123,  $\alpha$ Met42 and  $\beta$ Phe34). This swing takes no longer than 30 ps and the cleft in the channel is about 7 Å deep. After this ‘sidetrips’ ligands go back to the region between  $\beta$ Phe37 and  $\beta$ Phe41. From this position **ACN** (or **ACA**) can slide between  $\alpha$ Leu88 and the surface aminoacids:  $\beta$ Phe41,  $\beta$ Phe118,  $\beta$ Ala122,  $\beta$ Leu127 (see Fig. 4c and d). We observe that in this region of the SMD simulation substantial widening of the channel occurs. The distance between CZ\_ $\beta$ Phe41 and CG\_ $\beta$ Leu127 atoms increases from 6 to 10 Å (see blue lines in Fig. 4c and d). This widening is only weakly correlated with an increased force acting on ligands. At 0.8 ns ligands are already located in the NHase surface.

In order to check the effect of the selection of the SMD pulling force on calculated forces we performed four 2 ns simulations with the force vectors randomly oriented towards the protein matrix. These directions were approximately perpendicular to the channel axis. Two examples of such ‘brute-force’ dissociations are presented in Fig. 4e and f. Again, multiple maxima were observed, but the maximum forces are now of the order of 600–800 pN. To drag the ligand out of the protein takes much longer time: 1.2–1.5 ns, instead of 600–800 ps when the force is oriented along the channel.

The structural rearrangements of the enzyme channel exit are presented in Fig. 5. The crystallographic structure shows only a small entrance to the protein (Fig. 5a) but in all simulations, even after a heating phase, it is open (Fig. 5b). The size of the entrance increases further when the ligands are snaking between  $\beta$ Phe41 and  $\beta$ Leu127 (Fig. 5c). The opening (or closing) of the entrance can occur spontaneously – such an event was observed in the SMD simulation when a ligand was deep inside and in standard MD simulations, especially when **ACA** was studied.

Ligand–protein collision counts may help to identify the most important residues affecting transport and recognition properties of NHase. A collision was liberally defined as such an event when any ligand atom – protein atom distance becomes lower than 3 Å.

Collective normalized collision counts (26 ns data from all SMD runs) are presented in Fig. 6a. It can be seen that the most critical residues are:  $\beta$ Phe37,  $\alpha$ Leu88,  $\beta$ Leu127,  $\beta$ Ala122,  $\beta$ Phe118 and  $\beta$ Phe41. We were interested in qualitative differences between **ACN** and **ACA** interactions with the channel interior. Our limited

<sup>1</sup> For interpretation of color in figures, the reader is referred to the Web version of this article.



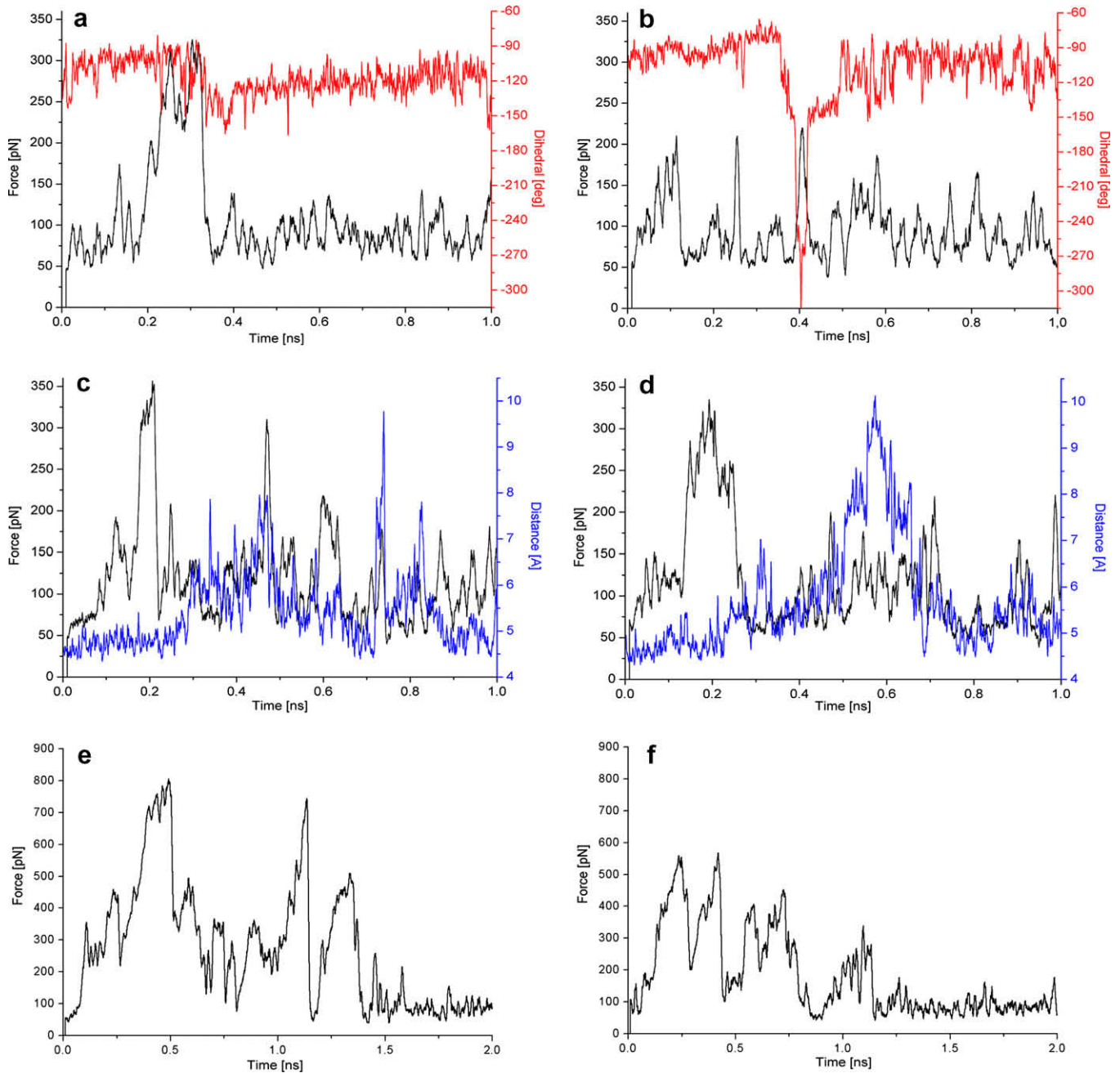


**Fig. 4.** Plots of forces (black) and dihedral angle CA-CB-CG-CD1 in  $\beta$ Phe37 for (a) ACN, (b) ACA, and CZ\_ $\beta$ Phe41-CG\_ $\beta$ Leu127 distance (c) in ACN, (d) ACA. Plots of forces observed in 'brute-force' (see text) dissociation of ACA (e,f).

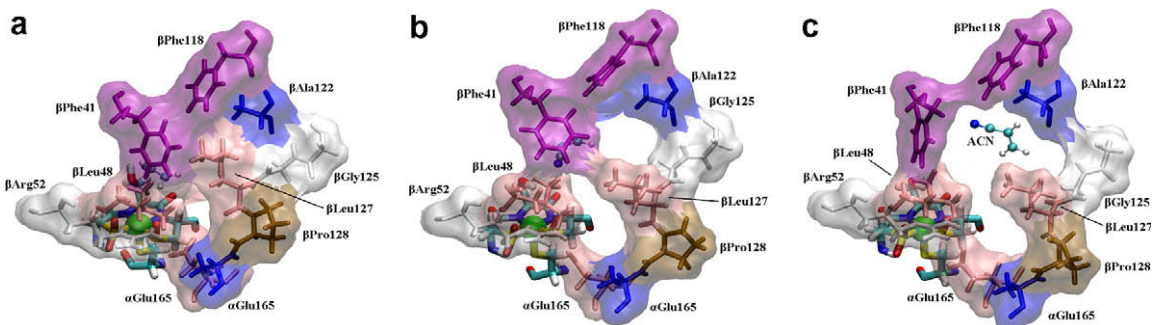


**Fig. 5.** A representation of the surface residues forming an entrance to the NHase channel in the crystallographic structure (a), after 100 ps heating (b), during the final SMD phase (c).

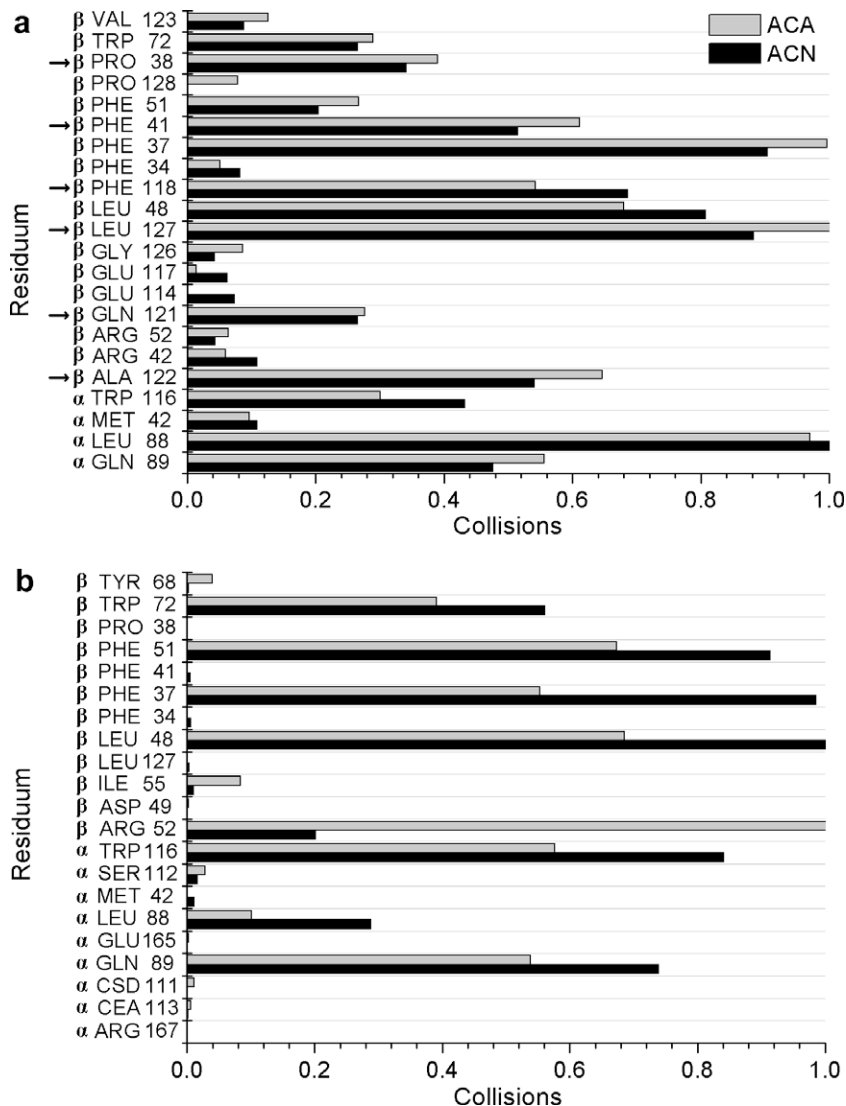


**Fig. 6.** Normalized number of collisions for ligands in all SMD simulations (a), in the first 10 ns of standard simulation (b). Aminoacids involved in steric interactions with ligands and revealed only in SMD simulations are indicated by arrows (a).

statistics indicate that interactions of **ACN** and **ACA** with the channel interior during the forced dissociation are quite similar. The largest difference is observed for  $\alpha$ Trp116 and it does not exceed 20% of the total collision count.

On the other hand, the differences in **ACN** and **ACA** collisions observed in the classical MD runs (Fig. 6b) are quite profound. The **ACA** product exhibits numerous contacts, mainly with  $\beta$ Arg52 and with a group of close lying aminoacids:  $\beta$ Leu48,  $\beta$ Phe51,  $\alpha$ Trp116,  $\beta$ Phe37,  $\alpha$ Gln89. Perhaps the higher collision count for  $\beta$ Arg52 is related to the formation of hydrogen bonds with the amide moiety of **ACA**. The **ACN** substrate interacts with this  $\beta$ Arg52 residue four times less frequently. At the same time it shows more frequent collisions with  $\beta$ Leu48,  $\beta$ Phe37,  $\alpha$ Trp116,  $\alpha$ Gln89 due to its higher mobility.

From Fig. 6 the advantage of using SMD in studies of large ligand transport in protein channels is clearly seen: while the histogram of collisions obtained for the classical 20 ns MD simulations (b) is composed of only 7 aminoacids located close to the Co-NHase center, the SMD part (a) shows twice as much aminoacids affecting transport of ligands on the whole solvent-catalytic site route. Thus, even the approximate SMD method is better suited to the identification of the candidate aminoacids for point muta-

tions, which may modulate the catalytic activity of the enzyme, than the classical simulations of an enzyme–ligand complex.

It is worth noting that the rms distances from the X-ray structure 1IRE for calculated trajectories did not exceed 2 Å. This shows that the unbinding forces of 300 pN are weak enough to be treated as small perturbations, and thus did not affect our NHase model.

#### 4. Conclusions

For the first time the biotechnologically important enzyme nitrile hydratase has been investigated using computer modelling and the CHARMM force field. The non-standard Steered MD method, with an external force applied to the docked substrate/product, has been used to generate plausible transport paths for a substrate **ACN** and the product **ACA**. The model NHase is stable during forced unbinding of ligands. The average unbinding force is of the order of 120 pN, while it is 80 pN when pulling a ligand through the bulk water. The maximum interaction forces (less than 300 pN), both for **ACN** and **ACA** are related to overcoming a steric barrier created by the  $\beta$ Phe37 residue. The brute-force dissociation of ligands in a random direction requires forces at least a factor of 2–3 higher.

Numerous collisions of ligands with this residue were observed both in SMD and classical trajectories. One may expect that this bulky phenylalanine plays a role in enantioselectivity of some NHases [31], since this aminoacid is weakly conserved in NHases sequences. Dynamical analysis of NHase reveals that the entrance to the protein may easily adopt a much larger size than that measured for the rigid X-ray structure. The aminoacids which interact very frequently with substrates and products of NHases were identified. In our opinion the SMD forced ligand–enzyme dissociation may be a source of useful hints for the new protein-engineered constructs of enzymes.

### Acknowledgements

This research was supported by Polish Ministry of Education and Science, Grant No. 2P04A 07229 (WN). LP acknowledges grant 'Krok w przyszłosc-stypendia dla doktorantow' supported by Marszałek Województwa Kujawsko-Pomorskiego.

### References

- [1] E.A. Galburt et al., *Nature* 446 (2007) 820.
- [2] M. Cieplak, *J. Phys.: Condens. Matter* 19 (2007) 1.
- [3] M. Cieplak, J.I. Sulkowska, *J. Chem. Phys.* 123 (2005) 194908.
- [4] P.E. Marszalek, H. Lu, H. Li, M. Carrion-Vazquez, A.F. Oberhauser, K. Schulten, J.M. Fernandez, *Nature* 402 (1999) 100.
- [5] G. Lee, K. Abdi, Y. Jiang, P. Michaely, V. Bennett, P.E. Marszalek, *Nature* 440 (2006) 246.
- [6] M. Sotomayor, K. Schulten, *Science* 316 (2007) 1144.
- [7] M. Sotomayor, V. Vasquez, E. Perozo, K. Schulten, *Biophys. J.* 92 (2007) 886.
- [8] B. Isralewitz, J. Baudry, J. Gullingsrud, D. Kosztin, K. Schulten, *J. Mol. Graph. Model.* 19 (2001) 13.
- [9] G. Lee, W. Nowak, J. Jaroniec, Q. Zhang, P.E. Marszalek, *Biophys. J.* 87 (2004) 1456.
- [10] W. Nowak, P.E. Marszalek, *Comp. Chem.: Rev. Curr. Trends* 9 (2005) 47.
- [11] G. Lee, W. Nowak, J. Jaroniec, Q. Zhang, P.E. Marszalek, *J. Am. Chem. Soc.* 126 (2004) 6218.
- [12] Z. Lu, W. Nowak, G. Lee, P.E. Marszalek, W. Yang, *J. Am. Chem. Soc.* 126 (2004) 9033.
- [13] M.O. Jensen, Y. Yin, E. Tajkhorshid, K. Schulten, *Biophys. J.* 93 (2007) 92.
- [14] M. Gao, H. Lu, K. Schulten, *Biophys. J.* 81 (2001) 2268.
- [15] M. Sotomayor, D.P. Corey, K. Schulten, *Structure* 13 (2005) 669.
- [16] W. Nowak, S. Wasilewski, L. Peplowski, NIC Series, vol. 36, John von Neumann Institute for Computing, 2007. p. 251.
- [17] H. Grubmuller, B. Heymann, P. Tavan, *Science* 271 (1996) 997.
- [18] D. Kosztin, S. Izrailev, K. Schulten, *Biophys. J.* 76 (1999) 188.
- [19] M. Francesca Gerini, D. Roccatano, E. Baciocchi, A. Di Nola, *Biophys. J.* 84 (2003) 3883.
- [20] L. Shen et al., *Biophys. J.* 84 (2003) 3547.
- [21] S.K. Ludemann, V. Lounnas, R.C. Wade, *J. Mol. Biol.* 303 (2000) 813.
- [22] X. Liu, X. Wang, H. Jiang, *J. Biochem. Biophys. Meth.* 70 (2008) 857.
- [23] M. Kobayashi, T. Nagasawa, H. Yamada, *Trends. Biotechnol.* 10 (1992) 402.
- [24] S.M. Thomas, R. DiCosimo, A. Nagarajan, *Trends. Biotechnol.* 20 (2002) 238.
- [25] W. Nowak, Y. Ohtsuka, J. Hasegawa, H. Nakatsuji, *Int. J. Quant. Chem.* 90 (2002) 1174.
- [26] S.N. Greene, N.G. Richards, *Inorg. Chem.* 45 (2006) 17.
- [27] S. Mitra, R.C. Holz, *J. Biol. Chem.* 282 (2007) 7397.
- [28] K.H. Hopmann, J.D. Guo, F. Himo, *Inorg. Chem.* 46 (2007) 4850.
- [29] K. Kubiak, W. Nowak, *Biophys. J.* 94 (2008) 3824.
- [30] T.C. Harrop, P.K. Mascharak, *Acc. Chem. Res.* 37 (2004) 253.
- [31] L. Martinkova, V. Kren, *Biocatal. Biotransform.* 20 (2002) 73.
- [32] A. Banerjee, R. Sharma, U.C. Banerjee, *Appl. Microbiol. Biotechnol.* 60 (2002) 33.
- [33] A. Miyanaga, S. Fushinobu, K. Ito, T. Wakagi, *Biochem. Biophys. Res. Commun.* 288 (2001) 1169.
- [34] L. Peplowski, K. Kubiak, W. Nowak, NIC Series, vol. 36, John von Neumann Institute for Computing, 2007. p. 259.
- [35] L.V. Desai, M. Zimmer, *Dalton Trans.* (2004) 872.
- [36] G.M. Morris, D.S. Goodsell, R.S. Halliday, R. Huey, W.E. Hart, R.K. Belew, A. Olson, *J. Comput. Chem.* 19 (1998) 1639.
- [37] L. Peplowski, K. Kubiak, W. Nowak, *J. Mol. Model.* 13 (2007) 725.
- [38] J.C. Phillips et al., *J. Comput. Chem.* 26 (2005) 1781.
- [39] A.D. MacKerell Jr. et al., *J. Phys. Chem. B* 102 (1998) 3586.
- [40] W. Humphrey, A. Dalke, K. Schulten, *J. Mol. Graph.* 14 (1996) 33.
- [41] L. Song, M. Wang, J. Shi, Z. Xue, M.X. Wang, S. Qian, *Biochem. Biophys. Res. Commun.* 362 (2007) 319.
- [42] W. Huang, J. Jia, J. Cummings, M. Nelson, G. Schneider, Y. Lindqvist, *Structure* 5 (1997) 691.
- [43] A.O. Tastan Bishop, T. Sewell, *Biochem. Biophys. Res. Commun.* 343 (2006) 319.
- [44] S. Nagashima et al., *Nat. Struct. Biol.* 5 (1998) 347.
- [45] L. Song, M. Wang, X. Yang, S. Qian, *Biotechnol. J.* 2 (2007) 717.